

Study of the ρ and ω meson decays into pseudoscalar meson and e^+e^- pair with the CMD-2 detector

R.R. Akhmetshin^a, V.M. Aulchenko^{a,c}, V.Sh. Banzarov^a,
 A. Baratt^d, L.M. Barkov^{a,c}, N.S. Bashtovoy^a, A.E. Bondar^{a,c},
 D.V. Bondarev^a, A.V. Bragin^a, S.I. Eidelman^{a,c},
 D.A. Epifanov^a, G.V. Fedotovitch^{a,c}, N.I. Gabyshev^a,
 D.A. Gorbachev^a, A.A. Grebeniuk^a, D.N. Grigoriev^{a,c},
 F.V. Ignatov^a, S.V. Karpov^a, V.F. Kazanin^{a,c}, B.I. Khazin^{a,c},
 I.A. Koop^{a,c}, P.P. Krovkovny^{a,c}, A.S. Kuzmin^{a,c},
 I.B. Logashenko^{a,b}, P.A. Lukin^a, A.P. Lysenko^a,
 K.Yu. Mikhailov^a, A.I. Milstein^{a,c}, I.N. Nesterenko^{a,c},
 M.A. Nikulin^{a,c}, V.S. Okhapkin^a, A.V. Otboev^a,
 E.A. Perevedentsev^{a,c}, A.A. Polunin^a, A.S. Popov^a,
 S.I. Redin^a, N.I. Root^a, A.A. Ruban^a, N.M. Ryskulov^a,
 A.G. Shamov^a, Yu.M. Shatunov^a, B.A. Shwartz^{a,c},
 A.L. Sibidanov^a, V.A. Sidorov^a, A.N. Skrinsky^a,
 I.G. Snopkov^a, E.P. Solodov^{a,c}, J.A. Thompson^{d 1},
 A.A. Valishev^a, Yu.V. Yudin^a, A.S. Zaitsev^{a,c}, S.G. Zverev^a

^a*Budker Institute of Nuclear Physics, Novosibirsk, 630090, Russia*

^b*Boston University, Boston, MA 02215, USA*

^c*Novosibirsk State University, Novosibirsk, 630090, Russia*

^d*University of Pittsburgh, Pittsburgh, PA 15260, USA*

Abstract

Using 3.3 pb^{-1} of data collected with the CMD-2 detector in the 720 – 840 MeV c.m. energy range, the branching fraction of the conversion decay $\omega \rightarrow \pi^0 e^+ e^-$ has been measured: $\mathcal{B}(\omega \rightarrow \pi^0 e^+ e^-) = (8.19 \pm 0.71 \pm 0.62) \cdot 10^{-4}$. The upper limits for the branching fractions of the following conversion decays have been obtained at the 90% confidence level: $\mathcal{B}(\rho \rightarrow \pi^0 e^+ e^-) < 1.6 \cdot 10^{-5}$, $\mathcal{B}(\rho \rightarrow \eta e^+ e^-) < 0.7 \cdot 10^{-5}$ and $\mathcal{B}(\omega \rightarrow \eta e^+ e^-) < 1.1 \cdot 10^{-5}$.

¹ deceased

Key words: CMD-2, light vector mesons, conversion decays

1 Introduction

Measurement of branching fractions and transition form factors of conversion decays provides an important test of vector dominance model [1,2] and an accurate background estimation in searches for quark-gluon plasma involving a lepton pair [3,4].

The expected branching fractions for the ρ and ω conversion decays are $\mathcal{B}(\omega \rightarrow \pi^0 e^+ e^-) = (7.2 - 8.0) \cdot 10^{-4}$, $\mathcal{B}(\rho \rightarrow \pi^0 e^+ e^-) = (4.1 - 6.5) \cdot 10^{-6}$ and an order of magnitude smaller for decays with muons and/or η meson in the final state [5,6,7]. Various conversion decays of the ϕ meson were studied at CMD-2 [8,9] and SND [10,11]. For the ρ and ω mesons experimental information is rather scarce: only the branching fractions for the decays $\omega \rightarrow \pi^0 e^+ e^-$ and $\omega \rightarrow \pi^0 \mu^+ \mu^-$ were measured in experiments at ND [12] and Lepton-G [13] with an accuracy $\sim 30\%$.

Conversion decays of a vector meson V into a pseudoscalar meson P and lepton pair $l^+ l^-$ ($V \rightarrow P l^+ l^-$) are closely related to the corresponding radiative meson decays $V \rightarrow P \gamma$ [5] and provide a possibility to study a transition $V \rightarrow P$ form factor, $F_{VP}(q^2)$, as a function of squared mass of virtual photon, $q^2 = M_{inv}^2(l^+ l^-)$.

In this work we present the result of the studies of the ρ and ω conversion decays into a $e^+ e^-$ pair and pseudoscalar meson (π or η) performed with the CMD-2 detector at the VEPP-2M collider [14]. The analysis is based on a data sample collected at 19 energy points in the 720 – 840 MeV c.m. energy range and corresponding to 3.3 pb^{-1} of integrated luminosity. This statistics contains about $3.3 \cdot 10^6$ ρ and $1.8 \cdot 10^6$ ω decays. More detailed description of this analysis can be found in [15].

2 Experiment

The general purpose detector CMD-2 has been described in detail elsewhere [16]. The tracking system consists of the cylindrical drift chamber (DC) with 250μ resolution transverse to the beam plane and double-layer multiwire proportional Z-chamber, both also used for the trigger. The tracking system is placed inside a thin ($0.38 X_0$) superconducting solenoid with a field of 1 T. The barrel CsI calorimeter with a thickness of $8.1 X_0$ placed outside the solenoid has

energy resolution for photons of about 9% in the energy range from 100 to 700 MeV. The angular resolution is of the order of 0.02 radians. The end-cap BGO calorimeter with a thickness of $13.4 X_0$ placed inside the solenoid has energy and angular resolution varying from 9% to 4% and from 0.03 to 0.02 radians, respectively, for the photon energy in the range 100 to 700 MeV. The barrel and end-cap calorimeter systems cover a solid angle of $0.92 \times 4\pi$ radians.

3 Data analysis

The decay $\omega \rightarrow \pi^0 e^+ e^-$ has been studied using the π^0 dominant decay mode $\pi^0 \rightarrow \gamma\gamma$. It corresponds to a final state with two opposite charge particles and two photons.

One of the significant resonant backgrounds comes from the $\omega \rightarrow \pi^+ \pi^- \pi^0$ decay which has the same topology of the final state and more than three orders of magnitude larger probability. Another source of resonant background is the $\omega \rightarrow \pi^0 \gamma$ decay followed by the Dalitz decay of the π^0 or γ -quantum conversion in the material in front of the drift chamber. Most conversions occur in the beam pipe, at the distance of 1.8 cm from the interaction point. Since the DC spatial resolution is not sufficient to separate events with conversions in the beam pipe from those where it occurs at the interaction point, the contribution of this background was subtracted based on Monte Carlo simulation (MC). The non-resonant background includes contributions from the following QED processes with the same final state topology: $e^+ e^- \rightarrow e^+ e^- \gamma\gamma$, $e^+ e^- \rightarrow 3\gamma$ followed by γ -quantum conversions, $e^+ e^- \rightarrow e^+ e^- \gamma$ with one background photon as well as two-quantum annihilation followed by a γ -quantum conversion and one background photon in calorimeters.

The data analysis consists of two parts: a measurement of the branching fraction and a study of the transition form factor. The selection criteria used for the measurement of the branching fractions were tuned to select a “pure” set of events under study and thus reject events with a large invariant mass of $e^+ e^-$ which contain a lot of background. However, this very range is of main interest for a study of the transition form factor. Therefore, for the latter a special set of selection criteria including a technique of e/π separation [9,17] was applied to suppress the main background from 3π events.

3.1 Selection of $\rho(\omega) \rightarrow \pi^0 e^+ e^-$ events

At the first stage of selection, the following criteria were applied to events with two tracks and at least two photons to enrich a data sample with events

of the studied decays:

- the photon energy $E_\gamma > 40$ MeV and its polar angle $0.5 < \theta_\gamma < \pi - 0.5$ to suppress background photons in the calorimeters;
- the impact parameter of the tracks $\rho < 1$ cm and Z-coordinate of the vertex $|Z_{vert}| < 5$ cm to reject cosmic rays and beam background events;
- the total momentum of the tracks $p = |\vec{P}_1 + \vec{P}_2|$ does not strongly differ from the photon momentum p_γ in the $\omega \rightarrow \pi^0\gamma$ decay at a given energy $|p - p_\gamma| < 35$ MeV/c to suppress $\omega \rightarrow \pi^+\pi^-\pi^0$ events as well as $\omega \rightarrow \pi^0\gamma$ events followed by the Dalitz decay of the π^0 . This condition is illustrated with horizontal lines in Fig. 1 where events satisfying previous requirements are shown;
- the angle between the total momentum of the tracks and each photon is more than 1.7 to suppress QED events;
- the invariant mass of the electron-positron pair and most energetic photon $M_{inv}(e^+e^-\gamma_1)$ is less than $1.9 \cdot E_{beam}$ to suppress $e^+e^- \rightarrow \gamma\gamma$ events followed by a conversion of one γ -quantum;
- the opening angle of the tracks $\Delta\psi < 0.5$ to suppress events of the $\omega \rightarrow \pi^+\pi^-\pi^0$ decay, this condition is shown in Fig. 1 with a vertical line.

Using these criteria 390 events were selected.

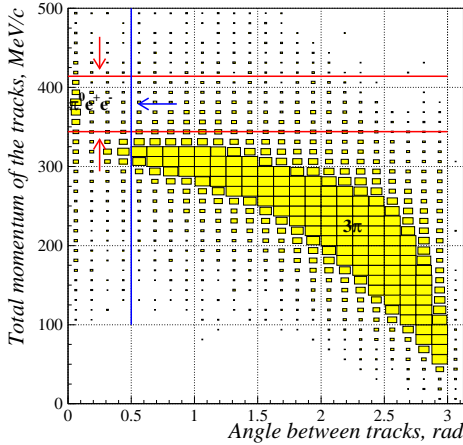


Fig. 1. Opening angle of two tracks $\Delta\psi$ versus their total momentum p . The horizontal lines show the cut on the total momentum and the vertical one shows the cut on the opening angle of the tracks.

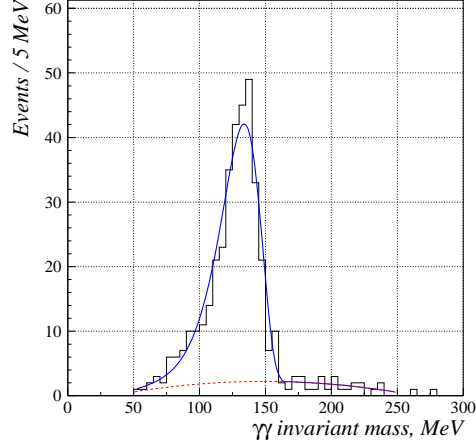


Fig. 2. The $M_{inv}(\gamma\gamma)$ distribution (histogram). The results of the fit are shown with a solid (signal) and dotted (background) line.

At the next stage, a fit of the $\gamma\gamma$ invariant mass distribution ($M_{inv}(\gamma\gamma)$) was performed at each energy point to determine the number of events with π^0 in the final state denoted hereafter as “ $\pi^0 2c$ ” ($\omega \rightarrow \pi^0 e^+ e^-$, $\omega \rightarrow \pi^0\gamma$ followed by

a γ -conversion and $\omega \rightarrow \pi^+\pi^-\pi^0$). The parameterization included a logarithmic Gaussian for the signal and a second order polynomial for the background. The shape of these functions was fixed, so the floating parameters were the numbers of events of each type only. The shape of background was taken from a study of the $M_{inv}(\gamma\gamma)$ distributions from the ω decays into $\pi^0\gamma$ and $\pi^+\pi^-\pi^0$ specially selected in the whole energy range. The shape of the signal was obtained from the fit of the $M_{inv}(\gamma\gamma)$ distribution over all selected events with floating parameters of the function describing the signal, see Fig. 2. The total number of selected $\pi^0\gamma$ events is 316.

3.2 Study of main background processes

At this stage of analysis the expected number of background events was evaluated using the $\Delta\psi$ distribution. Its difference for events of the process under study and those of background was employed in the analysis: the former are strongly peaked near zero while events coming from the $\omega \rightarrow \pi^+\pi^-\pi^0$ decay have a smooth wide distribution. Events of the $\omega \rightarrow \pi^0\gamma$ decay with conversion, which are also strongly peaked near zero, predominantly populate the angular range $\Delta\psi < 0.3$. The $\Delta\psi$ distribution for the data after imposing all selection conditions but that on $\Delta\psi$ is shown by crosses in Fig. 3. Using the modified requirement $0.3 < \Delta\psi < 0.9$ we reject most of the events coming from the $\omega \rightarrow \pi^0\gamma$ decay with conversion and keep events under study as well as background events from the $\omega \rightarrow \pi^+\pi^-\pi^0$ and QED. The MC $\Delta\psi$ distribution for the main background of $\omega \rightarrow \pi^+\pi^-\pi^0$ shown with a hatched histogram in Fig. 3 was approximated with a function $f(x) \sim x^\alpha$ with $\alpha = 1.63 \pm 0.10$ in the $\Delta\psi < 0.9$ angular range. The energy dependence of the number of events selected at the first stage (with modified requirements on $\Delta\psi$) was used to determine the number of $\omega \rightarrow \pi^+\pi^-\pi^0$ events.

To this end, the number of selected events at each point was written as

$$N_i = (\sigma_{\text{res}}(s_i) (1 + \delta_i) + \sigma_{QED}(s_i)) \cdot L_i, \quad (1)$$

where $\sigma_{QED}(s) = \sigma_{QED}^0 \cdot m_\omega^2/s$, $\sigma_{\text{res}}(s)$ is the cross section of the ω meson production at the squared c.m. energy s , L_i denotes the integrated luminosity at the i -th energy point, and δ_i is a radiative correction. The floating parameters are σ_{QED}^0 and σ_{res}^0 — cross section values at the resonance peak. The resulting number of resonance events was calculated as a sum over all energy points: $N_{\text{res}} = \sum \sigma_{\text{res}}(s_i) L_i (1 + \delta_i) = 210 \pm 17$. After subtraction of the $\omega \rightarrow \pi^0 e^+ e^-$ contribution, the number of $\pi^+\pi^-\pi^0$ events $N_{\pi^+\pi^-\pi^0} = 180 \pm 20$ in the $0.3 < \Delta\psi < 0.9$ range. The above description of the $\Delta\psi$ distribution was used to calculate the number of $\omega \rightarrow \pi^+\pi^-\pi^0$ events in the $\Delta\psi < 0.5$

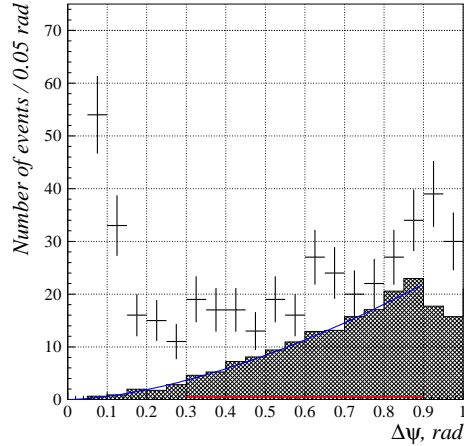


Fig. 3. The $\Delta\psi$ distribution for the data (crosses) and $\omega \rightarrow \pi^+\pi^-\pi^0$ simulation events (hatched histogram). All selection criteria but that on $\Delta\psi$ were applied. The number of $\pi^+\pi^-\pi^0$ MC events was approximated with a function x^α shown with a solid line.

range:

$$N_{3\pi} = 40.6 \pm 6.4 \pm 4.6. \quad (2)$$

The systematic error comes from the uncertainty of the $\Delta\psi$ distribution approximations and that of the subtraction of the $\omega \rightarrow \pi^0 e^+ e^-$ contribution. Since events of $\omega \rightarrow \pi^0 \gamma$ decays could not be distinguished from those under study, the detection efficiency for the former was determined as $\varepsilon_{\text{det}}^{\pi^0 e^+ e^-} \cdot P_{\text{conv}}$, where $\varepsilon_{\text{det}}^{\pi^0 e^+ e^-}$ denotes the detection efficiency for $\pi^0 e^+ e^-$ events and P_{conv} is a probability for a monoenergetic photon from the $\omega \rightarrow \pi^0 \gamma$ decay to convert in the material in front of DC. The P_{conv} value was obtained from simulation:

$$P_{\text{conv}} = (1.91 \pm 0.06) \cdot 10^{-3}. \quad (3)$$

The error of the P_{conv} value above comes from the uncertainties in a thickness and composition of materials in front of DC.

3.3 Approximation of $\pi^0 2c$ events

At the last stage of analysis, the energy dependence of the number of $\pi^0 2c$ events is fitted with a sum of the contributions from the $\omega \rightarrow \pi^0 e^+ e^-$, $\pi^+\pi^-\pi^0$, $\pi^0 \gamma$ decays and possibly remaining QED events:

$$N_{\pi^0 2c, i} = N_{\pi^0 e^+ e^-, i} + N_{\pi^0 \gamma, i} + N_{3\pi, i} + N_{QED, i}. \quad (4)$$

The number of $\pi^0 e^+ e^-$ events at the i -th energy point was described by the expression (5):

$$N_{\pi^0 e^+ e^-, i} = \sigma_{\pi^0 e^+ e^-}(s_i) L_i (1 + \delta_i) \varepsilon_{\text{det}, i}^{\pi^0 e^+ e^-} \varepsilon_{\Delta\psi, i} \varepsilon_{\text{trig}, i} \mathcal{B}(\pi^0 \rightarrow \gamma\gamma), \quad (5)$$

where L_i is an integrated luminosity, δ_i is a radiative correction, $\varepsilon_{\text{det}, i}^{\pi^0 e^+ e^-}$, $\varepsilon_{\Delta\psi, i}$, $\varepsilon_{\text{trig}, i}$ denote the detection efficiency, efficiency of the reconstruction of close tracks and trigger efficiency at the i -th energy point, respectively. The energy dependence of the Born cross section $\sigma_{\pi^0 e^+ e^-}(s)$ was written using the relativistic Breit-Wigner approach with the ρ and ω meson contributions:

$$\sigma_{\pi^0 e^+ e^-}(s) = \frac{q^3(s)}{s^{3/2}} \cdot |A_\rho(s) + A_\omega(s) + a_0|^2. \quad (6)$$

Here $q(s)$ is a phase space factor:

$$q(s) = \frac{\sqrt{s}}{2} \left(1 - \frac{m_{\pi^0}^2}{s}\right), \quad (7)$$

$A_V(s)$ is an amplitude of the vector meson V :

$$A_V(s) = \frac{m_V^2 \Gamma_V \sqrt{\sigma_V^0} f_V}{D_V(s) q^{3/2}(m_V^2)}, \quad (8)$$

and the additional constant a_0 in the amplitude describes a possible contribution of higher resonances. The quantities m_V and σ_V^0 are the vector meson mass and the cross section at its peak, respectively, with σ_V^0 calculated without taking into account other contributions, and $f_V = e^{i\phi_V}$ is a phase factor. To describe the ρ - ω interference, the model with energy-independent interference phases was used with ϕ_ω set to zero and $\phi_\rho = -13^\circ$ [18]. The $1/D_V(s)$ is a vector meson propagator described by the expression:

$$D_V(s) = m_V^2 - s - im_V \Gamma_V(s). \quad (9)$$

The quantities $\Gamma_V(s)$ and $\Gamma_V = \Gamma_V(m_V^2)$ are vector meson width at the squared c.m. energy s and at the vector meson mass, respectively.

The number of $\pi^0 \gamma$ events was written as

$$N_{\pi^0 \gamma, i} = \sigma_{\pi^0 \gamma}(s_i) L_i (1 + \delta_i^{\pi^0 \gamma}) \varepsilon_{\text{det}, i}^{\pi^0 e^+ e^-} P_{\text{conv}} \varepsilon_{\Delta\psi, i} \varepsilon_{\text{trig}, i} \mathcal{B}(\pi^0 \rightarrow \gamma\gamma), \quad (10)$$

with $\sigma_{\pi^0 \gamma}(s)$ taken from [18] and a photon conversion probability P_{conv} taken from (3). To describe the energy dependence of $\pi^+ \pi^- \pi^0$ events, the relativistic

Breit-Wigner with the ω meson contribution was used:

$$N_{3\pi,i} = \sigma_{\text{BW}}(s_i) L_i (1 + \delta_i^{3\pi}) \varepsilon_{3\pi}. \quad (11)$$

Since the total number of $\pi^+\pi^-\pi^0$ events was previously found, see expression (2), the normalization factor $\varepsilon_{3\pi}$ was determined from the sum $N_{3\pi} = \sum \sigma_{\text{BW}}(s_i) L_i (1 + \delta_i^{3\pi}) \varepsilon_{3\pi}$. A possible contribution of QED events which can, e.g., appear because of the incorrect background subtraction was evaluated from the following expression:

$$N_{\text{QED},i} = \sigma_{\text{QED}}^0 L_i \frac{m_\omega^2}{s_i}. \quad (12)$$

The detection efficiencies $\varepsilon_{\text{det},i}^{\pi^0 e^+ e^-}$ were determined using the Monte-Carlo simulation taking into account initial and final state radiation. The calculation of radiative corrections δ followed Ref. [19].

The events under study can be triggered by two independent triggers: charged and neutral ones. The overall trigger efficiency is estimated to be 99%. The estimation of this value has been performed by analysis of the trigger signals in selected events.

Since Monte-Carlo simulation does not completely describe the experiment, a correction $\varepsilon_{\Delta\psi}$ for a difference between the efficiencies of close track reconstruction in simulation and experiment was included to describe the data. Its value was obtained using events of $\omega \rightarrow \pi^+\pi^-\pi^0$ decays followed by the conversion decay $\pi^0 \rightarrow e^+e^-\gamma$ with a similar $\Delta\psi$ distribution. The integrated luminosity was determined using events of large angle Bhabha scattering with radiative corrections taken into account according to [20].

Table 1 shows the detailed information about experiment including efficiencies of detection, trigger and close track reconstruction together with the number of $\pi^0 2c$ events and visible cross section calculated from the following expression:

$$\sigma_{\pi^0 2c}^{\text{vis}} = \frac{N_{\pi^0 2c}^{\text{exp}}}{L (1 + \delta) \varepsilon_{\text{det}}^{\pi^0 e^+ e^-} \varepsilon_{\Delta\psi} \varepsilon_{\text{trig}} \mathcal{B}(\pi^0 \rightarrow \gamma\gamma)}. \quad (13)$$

The energy dependence of the number of $\pi^0 2c$ events was fitted using the maximum likelihood method. The minimization function is shown here:

$$\mathcal{L} = \sum_{i=1}^n \left(\frac{(N_{\pi^0 2c,i} - N_{\pi^0 2c,i}^{\text{exp}})^2}{\sigma_{\pm,i}^2} \right) + \frac{(\tilde{N}_{3\pi} - N_{3\pi})^2}{N_{3\pi}} + \frac{(\tilde{m}_\omega - m_\omega)^2}{\varepsilon(m_\omega)^2} + \frac{(\tilde{\Gamma}_\omega - \Gamma_\omega)^2}{\varepsilon(\Gamma_\omega)^2}, \quad (14)$$

Table 1

The energy, integrated luminosity, radiative correction, detection efficiency, the reconstruction efficiency of close tracks, trigger efficiency, number of $\pi^0 2c$ events and visible cross section of $\pi^0 2c$ events.

\sqrt{s} , MeV	L , nb $^{-1}$	δ	$\varepsilon_{\text{det}}^{\pi^0 e^+ e^-}$	$\varepsilon_{\Delta\psi}$	$\varepsilon_{\text{trig}}$	$N_{\pi^0 2c}^{\text{exp}}$	$\sigma_{\pi^0 2c}^{\text{vis}}$, nb
720	183.86	-0.099	0.149	0.906	0.989	$0.8_{-0.6}^{+1.2}$	$0.04_{-0.03}^{+0.06}$
750	148.66	-0.119	0.149	0.906	0.989	$1.5_{-0.9}^{+1.6}$	$0.09_{-0.06}^{+0.10}$
760	157.11	-0.152	0.149	0.906	0.989	$3.4_{-1.5}^{+2.2}$	$0.20_{-0.09}^{+0.13}$
770	45.81	-0.186	0.149	0.906	0.989	$0.0_{-0.0}^{+1.0}$	$0.00_{-0.00}^{+0.21}$
774	119.57	-0.211	0.148	0.906	0.989	$3.1_{-1.5}^{+2.1}$	$0.26_{-0.12}^{+0.17}$
778	128.25	-0.218	0.148	0.906	0.989	$19.4_{-4.4}^{+5.0}$	$1.50_{-0.34}^{+0.39}$
780	132.82	-0.229	0.148	0.906	0.989	$21.4_{-4.9}^{+5.1}$	$1.61_{-0.37}^{+0.38}$
781	187.09	-0.224	0.148	0.906	0.989	$28.8_{-5.3}^{+5.9}$	$1.52_{-0.28}^{+0.31}$
782	240.98	-0.211	0.148	0.906	0.989	$56.8_{-7.9}^{+8.5}$	$2.30_{-0.32}^{+0.34}$
783	187.34	-0.191	0.148	0.906	0.989	$54.1_{-7.6}^{+8.2}$	$2.77_{-0.39}^{+0.42}$
784	237.05	-0.167	0.149	0.906	0.995	$56.3_{-7.9}^{+8.4}$	$2.20_{-0.31}^{+0.33}$
785	191.51	-0.138	0.149	0.906	0.998	$35.0_{-5.6}^{+7.5}$	$1.63_{-0.26}^{+0.35}$
786	108.63	-0.112	0.149	0.906	0.998	$9.2_{-2.7}^{+3.4}$	$0.71_{-0.21}^{+0.26}$
790	117.03	0.053	0.149	0.906	0.998	$9.5_{-2.8}^{+3.4}$	$0.60_{-0.17}^{+0.22}$
794	121.81	0.260	0.149	0.906	0.998	$5.1_{-1.9}^{+2.6}$	$0.27_{-0.10}^{+0.14}$
800	195.50	0.427	0.150	0.907	0.998	$2.6_{-1.3}^{+2.0}$	$0.07_{-0.04}^{+0.06}$
810	181.17	0.828	0.151	0.907	0.998	$2.6_{-1.3}^{+2.0}$	$0.07_{-0.03}^{+0.05}$
820	185.52	1.023	0.151	0.907	0.998	$2.7_{-1.3}^{+2.0}$	$0.06_{-0.03}^{+0.05}$
840	457.87	1.260	0.151	0.907	0.998	$3.2_{-1.5}^{+2.1}$	$0.03_{-0.01}^{+0.02}$

where $N_{\pi^0 2c, i} = N_{\pi^0 e^+ e^-, i} + N_{\pi^0 \gamma, i} + N_{3\pi, i} + N_{QED, i}$ and $N_{\pi^0 2c, i}^{\text{exp}}$ is the experimental number of $\pi^0 2c$ events at the i -th energy point. The quantities $\sigma_{\pm, i}^2$ are asymmetric variances of the number of $\pi^0 2c$ events. The floating parameters are two branching fractions $\mathcal{B}(\omega \rightarrow \pi^0 e^+ e^-)$ and $\mathcal{B}(\rho \rightarrow \pi^0 e^+ e^-)$, and the constants a_0 and σ_{QED}^0 . Since the statistics is not sufficient to determine precisely main parameters of the ω meson, the fit allows ω meson mass \tilde{m}_ω , width $\tilde{\Gamma}_\omega$ and the number of $\pi^+ \pi^- \pi^0$ events $\tilde{N}_{3\pi}$ (three last terms in expression (14)) to float around their expected values within their estimated uncertainties. The central value and error m_ω and Γ_ω were taken from PDG [21] while those for $N_{3\pi}$ were taken from (2). The ρ meson parameters were fixed from the work [22].

Table 2

The fit results in various models. Only statistical errors are shown.

Model	$\mathcal{B}(\omega), 10^{-4}$	$\mathcal{B}(\rho), 10^{-4}$	$\sigma_{QED}, \text{ pb}$	$a_0, \text{ nb}^{1/2}$	$\chi^2/\text{n.d.f.}$
I	8.19 ± 0.81	fixed	-0.1 ± 2.5	$\equiv 0$	19.11/17
II	8.20 ± 0.77	fixed	$\equiv 0$	0.10 ± 0.14	18.17/17
III	8.19 ± 0.71	fixed	$\equiv 0$	$\equiv 0$	19.11/18
IV	8.33 ± 1.37	0.032 ± 0.081	$\equiv 0$	$\equiv 0$	19.06/17

Four different models were used. The ratio of σ_ω^0 and σ_ρ^0 values, cross sections at the ρ and ω meson peak, respectively, was fixed in some models from the results of the study of the process $e^+e^- \rightarrow \pi^0\gamma$ [18], so that

$$\frac{\sigma^0(\rho \rightarrow \pi^0 e^+ e^-)}{\sigma^0(\omega \rightarrow \pi^0 e^+ e^-)} \approx \frac{\sigma^0(\rho \rightarrow \pi^0 \gamma)}{\sigma^0(\omega \rightarrow \pi^0 \gamma)} = (3.7 \pm 1.0) \cdot 10^{-3}. \quad (15)$$

The theoretical precision of the approximate equality in (15) is evaluated as 3% for the applied selection criteria because of small q^2 in selected events. The expression (15) fixes the ratio between the branching fractions $\mathcal{B}(\rho \rightarrow \pi^0 e^+ e^-)/\mathcal{B}(\omega \rightarrow \pi^0 e^+ e^-) = (1.6 \pm 0.4) \cdot 10^{-3}$.

A fit in the first model was performed with floating σ_{QED}^0 to evaluate a possible contribution of QED events. As a result, the contribution of QED to $\pi^0 2c$ events is negligible, so in the other models this parameter was fixed to zero. Later, the fit in model II had a floating a_0 to evaluate a possible contribution from higher resonances. As a result, this contribution a_0 does not differ from zero within a statistical error. In model III a fit with a fixed ratio $\sigma_\rho^0/\sigma_\omega^0$ was performed to obtain a branching fraction for the $\omega \rightarrow \pi^0 e^+ e^-$ decay

$$\mathcal{B}(\omega \rightarrow \pi^0 e^+ e^-) = (8.19 \pm 0.71 \pm 0.62) \cdot 10^{-4}. \quad (16)$$

The graphical demonstration of this fit together with the visible cross section of the $\pi^0 2c$ events is shown in Figure 4. As a result of this fit the number of $\omega \rightarrow \pi^0 e^+ e^-$ events was determined to be 232. Finally, a fit in model IV with floating $\mathcal{B}(\omega \rightarrow \pi^0 e^+ e^-)$ and $\mathcal{B}(\rho \rightarrow \pi^0 e^+ e^-)$ was performed to set an upper limit on the branching fraction for the $\rho \rightarrow \pi^0 e^+ e^-$ decay:

$$\mathcal{B}(\rho \rightarrow \pi^0 e^+ e^-) < 1.6 \cdot 10^{-5} \text{ (90\% C.L.)}. \quad (17)$$

The obtained value of the $\omega \rightarrow \pi^0 e^+ e^-$ branching fraction (expression (16)) agrees with the previous measurement from ND [12] but has two times better accuracy. It is also consistent with the theoretical predictions [6,7].

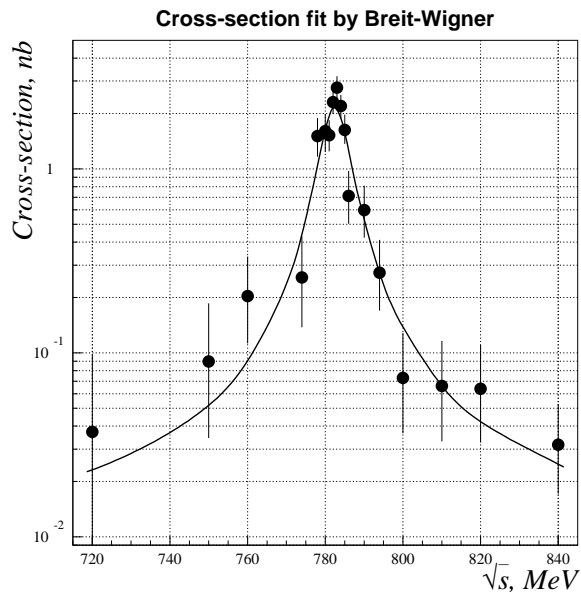


Fig. 4. Visible cross section of $\pi^0 2c$ events. The fit in model III is shown.

3.4 Systematic errors

The main sources of systematic uncertainties of the branching fractions are listed in Table 3. A contribution of each parameter to the total systematic er-

Table 3

The main sources of systematic uncertainties

Source	Uncertainty, %
Reconstruction efficiency of close tracks $\varepsilon_{\Delta\psi}$	4.7
Background subtraction	3.6
Detection efficiency $\varepsilon_{\text{det}}^{\pi^0 e^+ e^-}$	2.2
Trigger efficiency $\varepsilon_{\text{trig}}$	2.0
Parameters of ρ and ω	2.0
Mixing parameter $a = \sigma_\rho^0 / \sigma_\omega^0$	1.9
Integrated luminosity	1.4
Form factor model	1.2
Radiative corrections	1.2
Probability of conversion	1.0
Total	7.6

ror was estimated as a change of the branching fraction when this parameter

was varied within its measurement uncertainty. The main contribution comes from the reconstruction efficiency of close tracks and it is completely determined by statistics of the test samples of the $\omega \rightarrow \pi^+\pi^-\pi^0$ decays followed by $\pi^0 \rightarrow e^+e^-\gamma$. The background subtraction error originates from the inexact knowledge of the shape of the $M(\gamma\gamma)$ distribution for background events and from the error in the number of $\pi^+\pi^-\pi^0$ events. Since the reconstruction of close tracks is sensitive to the presence of the charged trigger, a contribution of the trigger efficiency was conservatively evaluated as a change of the branching fraction when we additionally demanded that the charged trigger was on. The detection efficiency error was determined by varying selection criteria. The uncertainty due to the determination of integrated luminosity comes from the selection criteria of Bhabha events, radiative corrections and calibration of the DC and CsI calorimeter. The uncertainty of the model of the transition form factor was evaluated by a difference in the detection efficiency when simple VDM with a single ρ meson as a transition particle and generalized VDM (ρ and ρ') were used in simulation. The uncertainty of radiative corrections comes from the dependence on the emitted photon energy and the accuracy of theoretical formulae. The resulting systematic uncertainty of the branching fraction quoted in Table 3 is 7.6%.

3.5 Search for ηe^+e^- events

A search was performed in three main decays modes of the η meson: $3\pi^0$, $\pi^+\pi^-\pi^0$ and 2γ . Selection criteria for a e^+e^- -pair were the same as for the $\pi^0 e^+e^-$ final state: $\rho < 1$ cm and $|Z_{vert}| < 5$ cm; the difference between the total momentum of the tracks $p = |\vec{p}_1 + \vec{p}_2|$ and the momentum p_γ in the $\omega \rightarrow \eta\gamma$ process at a given energy $|p - p_\gamma| < 30$ MeV/c; the opening angle of the tracks $\Delta\psi < 0.5$. In the $\eta \rightarrow \pi^+\pi^-\pi^0$ decay mode with a four-track final state a e^+e^- -pair was identified as a pair with opposite charges and the smallest opening angle. The following cuts on photons were applied:

- $\eta \rightarrow 3\pi^0$: the photon energy threshold was decreased to 30 MeV because of a higher multiplicity of soft photons in the final state, $N_\gamma \geq 5$;
- $\eta \rightarrow \pi^+\pi^-\pi^0$: $N_\gamma = 2$, $M_{inv}(e^+, e^-, \gamma_1)$, $M_{inv}(e^+, e^-, \gamma_2) > 160$ MeV/c² to suppress events from decays $\omega \rightarrow \pi^+\pi^-\pi^0$ followed by $\pi^0 \rightarrow e^+e^-\gamma$;
- $\eta \rightarrow 2\gamma$: $N_\gamma = 2$, the soft photon energy $E_{\gamma,2} > 175$ MeV to suppress QED events, $M_{inv}(e^+, e^-, \gamma_1)$, $M_{inv}(e^+, e^-, \gamma_2) > 200$ MeV/c² to suppress events from decays $\omega \rightarrow \pi^0\gamma$ followed by $\pi^0 \rightarrow e^+e^-\gamma$, the total momentum of the tracks and photons $P = |\vec{p}_1 + \vec{p}_2 + \vec{p}_{\gamma,1} + \vec{p}_{\gamma,2}| < 150$ MeV/c.

The main background for the $\eta \rightarrow \pi^+\pi^-\pi^0$ and $\eta \rightarrow 2\gamma$ decay modes comes from the QED processes while for the $\eta \rightarrow 3\pi^0$ decay mode it comes from the decay $\omega \rightarrow \pi^0\pi^0\gamma$ with a “fake” photon in calorimeters. The result of the

Table 4

The branching fraction, the detection efficiency at $s = m_\omega^2$, the reconstruction efficiency of close tracks, the trigger efficiency, the number of selected events and the average number of background events for analyzed η meson decay modes.

Decay mode	\mathcal{B} , %	ε_{det}	$\varepsilon_{\Delta\psi}$	$\varepsilon_{\text{trig}}$	N_{exp}	N_{back}
$\eta \rightarrow 3\pi^0$	32.51 ± 0.29	0.070	0.89	0.98	0	< 0.1
$\eta \rightarrow \pi^+\pi^-\pi^0$	22.6 ± 0.4	0.018	0.89	0.99	0	0.2
$\eta \rightarrow 2\gamma$	39.43 ± 0.26	0.059	0.89	0.98	3	4.9

analysis is shown in Table 4.

The total number of selected events for each η decay mode was expressed as:

$$N = \sum_{i=1}^n \sigma_{BW}(s_i) L_i (1 + \delta_i^{\eta e^+ e^-}) \varepsilon_{\text{det}}(s_i) \varepsilon_{\Delta\psi} \varepsilon_{\text{trig}} \mathcal{B}(\eta \rightarrow \text{final}). \quad (18)$$

The cross section parameterization is similar to formula (6) and includes relativistic Breit-Wigner contributions of the ρ and ω mesons, but without the a_0 term. The interference model with a constant phase $\phi_{\omega-\rho} = 0$ is used. We used the results of our study of the process $e^+e^- \rightarrow \eta\gamma$ [23] to fix the values of the amplitude: $\sigma^0(\rho \rightarrow \eta e^+ e^-) / \sigma^0(\omega \rightarrow \eta e^+ e^-) = 0.43 \pm 0.09$, from which the following relation between the branching fractions can be obtained: $\mathcal{B}(\rho \rightarrow \eta e^+ e^-) / \mathcal{B}(\omega \rightarrow \eta e^+ e^-) = 0.65 \pm 0.14$. Since the detection efficiency strongly depends on s , its value was calculated at each energy point. The radiative corrections $\delta^{\eta e^+ e^-}$, trigger efficiency $\varepsilon_{\text{trig}}$ as well as the reconstruction efficiency of close tracks $\varepsilon_{\Delta\psi}$ were calculated by the same method as for the $\pi^0 e^+ e^-$ events. The average number of background events has been evaluated by MC simulation. The simulation of corresponding events included generation of “fake” photons [24]. The results of all analyzed η decay modes are taken into account to calculate the upper limits on the branching fractions of the ρ and ω meson decays. The total number of selected events has been described by summation over expressions (18) applied to each η decay mode. To calculate upper limits, the Feldman-Cousins approach [25] was applied with 3 events observed and 5.1 background events expected. The final values of the upper limits were increased by 13% in accordance with the systematic error. The obtained upper limits exceed theoretical predictions by a factor of 2 [5,6,7]:

$$\mathcal{B}(\rho \rightarrow \eta e^+ e^-) < 0.7 \cdot 10^{-5} \text{ (90\% C.L.)}, \quad (19)$$

$$\mathcal{B}(\omega \rightarrow \eta e^+ e^-) < 1.1 \cdot 10^{-5} \text{ (90\% C.L.)}. \quad (20)$$

3.6 Study of the $\omega\pi$ transition form factor

The electromagnetic transition form factor $F(q^2)$ provides information on the electromagnetic structure of interacting particles. Its dependence on squared invariant mass of virtual photon q^2 can be approximated in a small q^2 range as

$$F(q^2) = 1 + b \cdot q^2, \quad (21)$$

where the parameter b is a slope of the transition form factor. In experiment the information about photon virtuality in events of $\omega \rightarrow \pi^0 e^+ e^-$ decay could be taken from the invariant mass of the lepton pair $M_{inv}(e^+ e^-) = q^2$. Since the previously used selection criteria leave events with small q^2 only and the detection efficiency strongly depends on $M_{inv}(e^+ e^-)$, the cuts on total momentum, angle between the total momentum of tracks and photons, $M_{inv}(e^+ e^- \gamma_1)$ were omitted and the cut on $\Delta\psi$ was increased up to 2.5 radians. To suppress background mainly originating from $\omega \rightarrow \pi^+ \pi^- \pi^0$, the kinematic fit requiring energy-momentum conservation and the procedure of e/π separation based on the energy deposition of charged particles in calorimeters [9,17] were additionally used.

The selected events were divided into groups of $M_{inv}(e^+ e^-)$. The number of $\omega \rightarrow \pi^0 e^+ e^-$ events in each group was determined from the analysis of the $\gamma\gamma$ invariant mass distribution. After that the q^2 dependence of the obtained number of events was fitted to the following function from [5]

$$\begin{aligned} \frac{dN}{dq} = & 2q \cdot A \cdot \frac{\alpha}{3\pi} \cdot \left(1 - \frac{4m_e^2}{q^2}\right)^{1/2} \cdot \left(1 + \frac{2m_e^2}{q^2}\right) \cdot \frac{1}{q^2} \times \\ & \times \left[\left(1 + \frac{q^2}{m_\omega^2 - m_\pi^2}\right)^2 - \frac{4m_\omega^2 q^2}{(m_\omega^2 - m_\pi^2)^2} \right]^{3/2} \cdot |F_{\omega\pi}(q^2)|^2, \end{aligned} \quad (22)$$

where α is the fine structure constant. The detector resolution on invariant mass $\sigma_q = 15 \text{ MeV}/c^2$ was taken into account. The floating parameters are the normalization factor A and the slope of the transition form factor b . The result of the fit is shown in Fig. 5, the slope value $b = 2.5 \pm 3.1 \text{ GeV}^{-2}$. The total systematic error is estimated to be 10%. The main contributions to it are the e/π separation procedure and selection criteria. This error is smaller than a statistical one for all invariant mass groups except for the group with $q < 50 \text{ MeV}/c^2$. The obtained value agrees with the VDM prediction $b = 1/m_\rho^2 = 1.7 \text{ GeV}^{-2}$ within statistical errors.

It is worth noting that modes with $\mu^+ \mu^-$ in the final state are more convenient for studies of the transition form factor $|F_{VP}(q^2)|$ [13]. Unfortunately, their

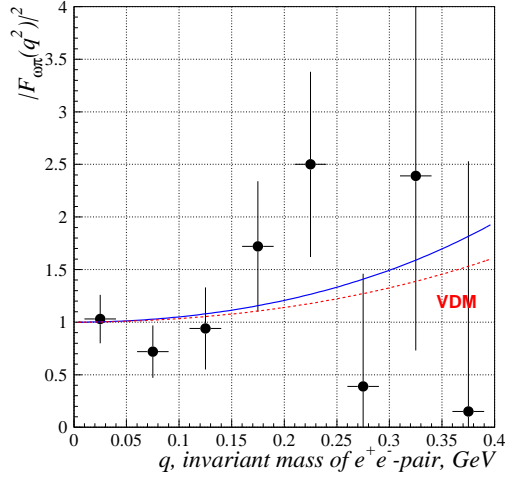


Fig. 5. Results of the fit of the data (dots with error bars) on the electromagnetic $\omega\pi$ transition form factor $|F(q^2)|^2$ (solid line). The VDM form factor is shown with a dotted line.

study at CMD-2 is complicated because of the large background coming from the dominant decay mode of the ω meson: $\omega \rightarrow \pi^+\pi^-\pi^0$ and insufficiently powerful μ/π separation at low momenta.

4 Conclusions

Using a data sample of 3.3 pb^{-1} in the 720 – 840 MeV c.m. energy range, the branching fraction for the $\omega \rightarrow \pi^0 e^+ e^-$ decay has been obtained:

$$\mathcal{B}(\omega \rightarrow \pi^0 e^+ e^-) = (8.19 \pm 0.71 \pm 0.62) \cdot 10^{-4}$$

and the following 90% C.L. upper limits were set:

$$\begin{aligned} \mathcal{B}(\rho \rightarrow \pi^0 e^+ e^-) &< 1.6 \cdot 10^{-5}, \\ \mathcal{B}(\rho \rightarrow \eta e^+ e^-) &< 0.7 \cdot 10^{-5}, \\ \mathcal{B}(\omega \rightarrow \eta e^+ e^-) &< 1.1 \cdot 10^{-5}. \end{aligned}$$

Acknowledgment

The authors are grateful to the staff of VEPP-2M for excellent performance of the collider, and to all engineers and technicians who participated in the design, commissioning and operation of CMD-2. This work is supported in part by grants DOE DEFG0291ER40646, NSF PHY-0100468, PST.CLG.980342,

RFBR-03-02-16280-a, RFBR-03-02-16477, RFBR-03-02-16843, RFBR-04-02-16217, RFBR-04-02-16233-a, and RFBR-04-02-16434.

References

- [1] T. H. Bauer *et al.*, Rev. Mod. Phys. **50** (1978) 261.
- [2] P. J. O'Donnell, Rev. Mod. Phys. **53** (1981) 673.
- [3] E. V. Shuryak, Phys. Lett. **B 78** (1978).
- [4] D. Adamova *et al.*, Phys. Rev. Lett. **91** (2003) 042301.
- [5] L. Landsberg, Phys. Rep. **128** (1985) 301.
- [6] S. I. Eidelman, Proceedings of the Workshop on Physics and Detectors for DAFNE, Frascati, Italy, April 1991, p.451.
- [7] A. Faessler *et al.*, Phys. Rev. **C 61** (2000) 261.
- [8] R. R. Akhmetshin *et al.*, Phys. Lett. **B 501** (2001) 191.
- [9] R. R. Akhmetshin *et al.*, Phys. Lett. **B 503** (2001) 237.
- [10] M. N. Achasov *et al.*, Phys. Lett. **B 504** (2001) 275.
- [11] M. N. Achasov *et al.*, JETP Lett. **75** (2002) 449.
- [12] S. I. Dolinsky *et al.*, Z. Phys. **C 42** (1989) 511.
- [13] R. I. Dzhelyadin *et al.*, Phys. Lett. **B 84** (1979) 143.
- [14] V. V. Anashin *et al.*, Preprint Budker INP **84-114**, Novosibirsk, 1984.
- [15] R. R. Akhmetshin *et al.*, Preprint Budker INP **2004-92**, Novosibirsk, 2004.
- [16] G. A. Aksenov *et al.*, Preprint Budker INP **85-118**, Novosibirsk, 1985.
E. V. Anashkin *et al.*, ICFA Instr. Bulletin **5** (1988) 18.
- [17] R. R. Akhmetshin *et al.*, Phys. Lett. **B 475** (2000) 190.
- [18] M. N. Achasov *et al.*, Phys. Lett. **B 559** (2003) 171.
- [19] E. A. Kuraev and V. S. Fadin, Sov. J. Nucl. Phys., **41** (1985) 466.
- [20] A. B. Arbuzov *et al.*, J. High Energy Phys., **10** (1997) 001.
- [21] S. Eidelman *et al.*, Phys. Lett. **B 592** (2004) 1.
- [22] R. R. Akhmetshin *et al.*, Phys. Lett. **B 578** (2004) 285.
- [23] R. R. Akhmetshin *et al.*, Phys. Lett. **B 509** (2001) 217.
- [24] P. P. Krokovny, Master's Thesis, Novosibirsk State University, 2000.
- [25] G. J. Feldman and R. D. Cousins, Phys. Rev. **D 57** (1998) 3873.